Gain Calibration of CCD Systems at VBO

T.P. Prabhu,Y.D. Mayya[1] & G. C. Anupama[2] *Indian Institute of Astrophysics, Bangalore 560034*

Abstract. The system gain of two CCD systems in regular use at the Vainu Bappu Observatory, Kavalur, is determined at a few gain settings. The procedure used for the determination of system gain and base-level noise is described in detail. The Photometrics CCD system at the 1-m reflector uses a Thomson-CSF TH 7882 CDA chip coated for increased ultraviolet sensitivity. The gain is programme-selected through the parameter 'cgain' varying between 0 and 4095 in steps of 1. The inverse system gain for this system varies almost linearly from 27.7 electrons DN^{-1} at cgain = 0 to 1.5 electrons DN^{-1} at cgain = 500. The readout noise is $\lesssim$ 11 electrons at cgain = 66. The Astromed CCD system at 2.3-m Vainu Bappu Telescope uses a GEC P8603 chip which is also coated for enhanced ultraviolet sensitivity. The amplifier gain is selected in discrete steps using switches in the controller. The inverse system gain is 4.15 electrons DN^{-1} at the gain setting of 9.2, and the readout noise $\sim$ 8 electrons.

Key words: CCD photometry—CCD spectroscopy—system gain—readout noise

1. Introduction

The charge-coupled device (CCD) is increasingly favoured for astronomical observations in the optical and near-infrared domains because of its sensitivity, linearity and dynamic range. It is also a reuseable detector and hence can be calibrated accurately. Its applications are limited at present only by the small format in which the detector is available. A CCD is an analog device. The charge (q) accumulated in a CCD pixel is converted to voltage ($qA/C_0 = V_0$) where C_0 is the output node capacitance, and A the voltage gain of the amplifier. An analog-to-digital converter (ADC) digitizes the voltage such that a specific voltage V_m is converted to a specific number of bits. The full-well capacity of some CCD chips exceeds 500,000 electrons (McLean 1989). If one chooses to set the amplifier gain such that one electronic charge results in one count or 'data number' (DN), an ADC with 19 bits will be needed to realize the full-well capacity. It is easier to use an ADC with 14–16 bits, which, at 1 electron DN^{-1}, will utilize only 313 per cent of the dynamic range.

The accuracy of detection of charge accumulated on the CCD is limited by the noise introduced in the process of measurement (the readout). The readout noise is in the range of 510 electrons for a majority of CCD chips currently used in astronomy (McLean 1989). There is no advantage in operating a CCD at gains much larger than one DN per readout noise. Most of the dynamic range of a typical CCD chip—defined as (full-well capacity)/(readout noise)—can be accommodated in 16 bits at one DN per readout noise. This setting is also optimal for the astronomical applications which range from background-noise-limited observations such as broad-band imaging where the sky background needs to be detected with significant accuracy (minimum detected signal » readout noise), and readout-noise-limited detection such as spectroscopy and speckle interferometry (minimum detected signal ≲ readout noise).

The system gain or transfer factor is defined as the value of DN per electronic charge detected. We denote this by the symbol G in the following. Often its inverse is also used in the units of electrons DN^{-1}, and we denote this value by Q. A count or DN is referred to in the literature also as an analog-to-digital unit (ADU) or an analog-to-digital count unit (ADCU). Q is sometimes referred as EPADU (electrons per ADU). The system gain needs to be calibrated for different values of amplifier gains so that an optimal setting may be determined. In addition, it is desirable to know its value for each observation, so that one can determine the scale factor between the observed counts and detected electrons. Simple procedures to do this will be useful in monitoring the long-term stability of the system. The information on the system gain and readout noise are necessary for estimating the total noise at any observed signal level, and are demanded by the standard software for reductions of CCD spectroscopy and photometry.

The system gain can be computed if the capacitance at the output node, the voltage gain of the amplifier, and the conversion factor at the ADC are known. On the other hand, it can easily be determined experimentally (*cf.,* Djorgovski 1984; Mackay 1986; Home 1988; McLean 1989; McCall, English & Shelton 1989). We have examined the experimental methods of calibrating the gain and readout noise of a CCD system, and tried to evolve a simple and accurate method using flats obtained routinely during spectroscopic observations. New commands have been added to the RESPECT software (Prabhu & Anupama 1991) for analysis of these spectroscopic flats.

Two CCD systems are available at VBO and each one is used both for imaging and spectroscopy. The 1-m Zeiss reflector is equipped with the CH210 camera head containing a Thomson CSF TH 7882 CDA chip coated for enhanced sensitivity in the ultraviolet, CE200 controller, and DIPS 1000 image acquisition and processing system, obtained from Photometrics Ltd., Tucson (USA) in 1988. The photometric calibration of this system has been performed by Sagar & Pati (1989) and Mayya (1991). The 2.3-m Vainu Bappu Telescope (VBT) is equipped with a CCD dewar and controller obtained from Astromed Inc., Cambridge (UK) in 1988 as CCD 2000 imaging system. It is equipped with a GEC P8603 CCD chip coated for enhanced ultraviolet sensitivity which replaced the original chip in 1991 January. A nearly identical system jointly belonging to TIFR, Bombay, and IUCAA, Pune (Bhat *et al.* 1990) is also available, and is used interchangeably. The data acquisition software currently in use was developed locally for this system using a personal computer (Ananth *et al.* 1991). We present new results on the calibration of these systems for system gain and readout noise in Section 3, after explaining the methodology in Section 2. The last section summarizes the conclusions.

2. The methodology

The gain calibration of a CCD system can be effected by studying its noise characteristics. In a unit integration period, N_e electrons are accumulated on a typical pixel as given by

$$N_e = b_e + d_e + fS_e,$$

where b_e is the DC offset ('bias') applied (in units of electronic charge) to avoid negative signal caused by fluctuations due to noise, d_e is the number of thermal electrons generated, and S_e is the number of electrons generated due to signal photons. The factor f varies from pixel to pixel, and denotes the relative quantum efficiency. If G denotes DN corresponding to one electron, the equation can be rewritten as

$$N_c = N_e G = b_c + d_c + fS_c,$$

where N_c, b_c, d_c, and S_c are in units of DN. The mean and variance of observed counts for a uniform illumination can be written as

$$\langle N_c \rangle = b_c + d_c + \langle S_c \rangle, \tag{1}$$

and

$$\sigma^2 = G^2 B_e^2 + G(d_c + S_c) + \sigma_f^2 S_c^2, \tag{2}$$

where B_e is the base-level noise in electrons and equals the sum in quadrature of the readout noise (R_e) and noise from other signal-independent sources (Newberry 1991). In deriving Equation (2) we have assumed that the noise in electrons generated thermally as well as due to the signal is Poissonian. The noise in signal electrons equals $\sqrt{S_e}$ electrons (*cf,* Newberry 1991), and hence the noise in the signal counts is $G\sqrt{S_e} = \sqrt{GS_e}$ counts. We also assume that the mean value of f is unity (definition). In the following, we drop the angular brackets for simplicity. We will also assume that the mean thermal counts and bias have been subtracted from the data and the the rms thermal noise has been subtracted from the derived noise. Most CCD chips currently available have very low thermal charge, and hence also its variance, at liquid nitrogen temperatures. Equation (2) can thus be written as

$$\sigma^2 = G^2 B_e^2 + GS_c + \sigma_f^2 S_c^2. \tag{3}$$

It is clear from Equation (3) that it is possible to determine G and B_e using a set of observed, bias- and dark-subtracted, signal counts (S_c) and their rms scatter (σ), sometimes referred to as the variance diagram. A set of flat-field images obtained at a range of illumination levels (or equivalently exposure times) can be used to this end. A quadratic fit to the data yields all the constants in Equation (3). In practice, the the propagation of errors downwards, *i.e.,* $\varepsilon(\sigma_f^2 G^2) \ll \varepsilon(G) \ll \varepsilon(G^2 B_e^2)$. This problem can be alleviated by the procedures described below.

2.1 *Reducing the Magnitude of the Quadratic Term*

The accuracy of determination of G in Equation (3) can be enhanced by reducing the magnitude of the third term in the equation. The quadratic term arises due to pixel-to-pixel sensitivity variations as also the non-uniformity of illumination in the

flat-field. Its magnitude can hence be reduced by correcting for these effects. We consider below two methods of reducing the effect of the quadratic term.

2.1.1 *Correcting for the flatfield variations*

The most accurate way of reducing the flat-field variations is to correct for them by using an accurate flat-field frame. In practice, it is not possible to correct for pixel-to-pixel variations exactly but only to a desired accuracy. If one desires that the third term in Equation (3) should not be larger than the second term even at the largest values of S_c, one obtains the condition that $\sigma_f \lesssim [G/S_c(\max)]^{1/2} = S_e\,(\max)^{-1/2}$, where σ_f is the residual flat-field variation. For a signal reaching the full-well capacity of 10^5 electrons, this implies that the flat-field corrections should be carried out to an accuracy of 0.3 per cent in order to achieve 1 per cent accuracy in σ_f. Many flats need to be stacked to obtain a master flat accurate to this level. It should be noted that the individual images used for obtaining the master flat cannot be used to study the noise statistics since the master contains the memory of the noise in individual flats. The corrected flats would, in such a case, show a lower-than-real noise. An independent set of flats, corrected using the master flat, should be used to determine the noise statistics. A quadratic fit of Equation (3) would still be necessary for the determination of G, though the constant σ_f^2 would now be very small. An example of this procedure is given by Horne (1988).

2.1.2 *Division or subtraction of two flats*

An alternative method of reducing the effect of flat-field noise is dividing two flat-field images after subtracting bias and dark. Mackay (1986) suggests dividing two equally exposed flats. In general, for two unequal flat-field images with mean counts S_1 and S_2, the variance of the divided image is

$$\sigma^2(S_1/S_2) = [S_2^2\sigma^2(S_1) + S_1^2\sigma^2(S_2)]/S_2^4. \tag{4}$$

A relationship similar to Equation (3) can now be written as

$$\sigma'^2 = G^2 B^2 + GS', \tag{5}$$

where

$$\sigma'^2 = \frac{S_2^4}{S_1^2 + S_2^2}\sigma^2\left(\frac{S_1}{S_2}\right),$$

and

$$S' = \frac{S_1 S_2 (S_1 + S_2)}{S_1^2 + S_2^2}.$$

The simplification for $S_1 = S_2$ is evident. Since the flat-field variations are not random, but affect both the frames the same way, the division does not contain the quadratic term $(\sigma_f(S_1 / S_2) = 0)$.

The propagation of errors due to normal flat-fielding operation is evident from Equation (5), since flat-fielding of image 1 involves division by image 2 such that $S_2 \gg S_1$. In practice, to restrict the relative error to e one requires $S_1/S_2 \ll \varepsilon^2$. On the other hand, Equation (5) is more general, and can be used for any ratio image.

The flat-field noise can also be eliminated by subtracting two equal flat-field images. If the two images are not exposed equally, it will become necessary to normalize

individual flats before subtraction. Denoting the normalized counts by *s*. The variance of the 'normalized difference image' can be expressed as

$$\sigma^2(s_1 - s_2) = \frac{\sigma^2(S_1)}{S_1^2} + \frac{\sigma^2(S_2)}{S_2^2}.$$

(6)

Equation (5) is valid in this case too, with

$$\sigma'^2 = \left(\frac{S_1^2 S_2^2}{S_1^2 + S_2^2}\right)\sigma^2(s_1 - s_2).$$

(7)

Again, the simplification for $S_1 = S_2$ is evident.

2.2 *Improving the Estimates of G and B*

The methods described in Section 2.1 reduced the magnitude of the quadratic term in Equation (3) and make it possible to determine the value of *G* accurately. However, the value of *B* determined by a least-squares polynomial fit would still be inaccurate since the linear term dominates. It is possible to improve the initial estimates of *G* and *B* obtained through usual least-squares analysis by iterative methods such as the Marquardt algorithm (*cf.*, Press *et al.* 1986). If the nonlinear term is small or absent, one can use a linear regression for initial estimates, and obtain the best fit by iteration.

The Marquardt algorithm is best suited for a minimization of χ^2 which requires an accurate model of the variance of the dependent variable. In the case of Equation (3), it is difficult to model the variance of σ^2, but its magnitude can be minimized by choosing a sufficiently large area to determine σ^2. We used Marquardt algorithm minimizing rms deviations, or equivalently, by assuming equal variance for all values of σ^2. Here again, it was seen that *B* cannot be determined accurately since the algorithm tries to fit larger values of σ^2 better. The problem can be alleviated, albeit rather arbitrarily, by obtaining the logarithm of Equation (3) and assigning equal weights to log σ^2 since now the weights get distributed more evenly. This representation has been in regular use (*cf.,* Horne 1988; McLean 1989). Though it does not have the rigour of a χ^2 fit, it yields a very good fit to the data.

2.3 *Analysis of Spectroscopic Flats*

Low-resolution spectroscopic flats often contain a range of signal levels due to the variation of instrumental response. Hence the division of two spectroscopic flats provides an easy way of constructing the variance diagram. We have set up a procedure to calibrate CCDs using low-resolution spectroscopic flats and the RESPECT software. The use of RESPCET software for spectroscopic data reduction has been described in detail by Prabhu & Anupama (1991). Here we describe the commands added more recently for gain calibration using the methods outlined above.

The command GSTAT determines the noise statistics based on two flats. The format of the command is

GSTAT flat l flat2 output.

The output contains mean counts and variances as (x, y) pairs. In the case of spectroscopic flats the programme automatically locates the spectrum, and evaluates the statistics using (10, 20) size boxes centred on the spectrum, spaced 10 pixels apart, The spectroscopic flats used here were about 40 pixels wide. The direction of dispersion (x direction) is assumed to be along columns. If it is along the rows, the information can be supplied through the qualifier/X = ROW. The box-size can be varied by the qualifier/BSIZE = (IX, IY). If one wishes to avoid some rows at the beginning and end of the spectrum, one can specify it as /XLIM = (X1, X2). The automatic centring of the boxes can be circumvented through explicit positioning by /YLIM = (Yl, Y2). If a mean bias value is to be subtracted from the data, one may do so with /MBIAS = const. Alternatively, one can input a bias frame as /BIAS = bias-frame. In this case, the mean value of bias is computed and subtracted. Further, the mean value is subtracted from the bias frame itself, boxes are centred on it at the same locations as on flats, and the mean and variance of these boxes are determined and added to the output file. These would help in fixing the readout noise better. It should be noted that the mean value of bias should actually be zero. Since this implies $\log S = -\infty$, and it is not possible to plot it in the logarithmic representation of the variance diagram, the absolute value of (local mean – global mean) is used as the mean value of S with the value $S < 0.01$ being discarded. This is only a matter of convenience, and has no effect on the final results.

The noise and variance are computed as transformed by Equations (5) and (7), By default, the first frame is divided by the second, and Equation (5) is used. If subtraction is desired, one should add/MODE = SUB.

The system gain and the readout noise are determined through the command GFIT input curve.

The input is the output of GSTAT command. The resultant coefficients of the linear or quadratic fit and the standard errors are printed in the log file. The theoretical fit is computed over the entire range of values and stored for future display in the file 'curve'. A linear relation transformed to the log-log domain is fitted by default. If a quadratic term is to be added, one uses/QUAD. A fit can also be obtained without using the logarithmic representation, with the qualifier/NOLOG.

3. Results

The two CCD systems in regular use at VBO were calibrated using the methods discussed above. The results are presented below.

3.1 *The Photometrics System*

The Photometrics CCD system at the 1-m reflector was calibrated in a greater detail compared to the Astromed system described in the following section. The system is in regular use since 1988. The noise statistics for the system were determined using the imaging flats at two different gain settings and spectroscopic flats at five different gain settings. No preflashing was employed in any of the observations.

The R band twilight sky flat images obtained during the imaging observations of 1991 April 16 and May 16 were used in the analysis. In addition to well-exposed flats

obtained routinely during observations, additional graded flats were obtained to uniformly cover lower signal levels. The gain setting 'cgain' = 0 was used in April, whereas a value of 33 was used in May. The first four rows and columns were trimmed since some of these showed abnormally low or high counts. The bias frames showed only faint strips which were not repeatable and hence only a mean bias value was subtracted from all the frames. A set of flats were stacked to obtain a master flat accurate to ~ 0.1 per cent. The remaining flats were corrected for pixel-to-pixel sensitivity variations, as also for the vignetting in the system, using the master flat. An area of the corrected flat enclosed by the rows (201, 500) and columns (101, 300) was used for determining the statistics, since this area was less affected by vignetting. The mean signal counts were determined from the flats before correction, in order to represent the signal accurately before the correction for vignetting. The rms noise was estimated over contiguous boxes of 5×5 pixels after rejection of deviants over three iterations.This procedure determines the local variance and should be relatively free of errors due to incomplete flat-field corrections. The EDRS subpackage of STARLINK software was used in all the reductions.

The spectroscopic flats were obtained during regular observing runs of 1991–92, using the Cassegrain UAG spectrograph and a 1501 mm^{-1} grating blazed at 8000 Å in the first order. Flat and bias frames at 'cgain' = 0 and 33 were obtained as a part of the observing programme, and a cgain = 66, 100 and 500 were obtained specifically for calibration of the system. The closed shutters of the dome, illuminated by incandescent lamps, were used as the continuum source. The grating setting corresponded to the wavelength range of 4200–7400 Å on April 17 (cgain = 0) and May 12 (cgain = 33), and 6000–9200 Å on May 13 (cgain = 66). On 1992 January 7 flats were obtained at three different grating settings: 3800–7000 Å (cgain = 33), 4200–7400 Å (cgain = 33, 100, 500), and 6300–9500 Å (cgain = 33). In general two equal, well-exposed flats were used in obtaining the noise statistics, though on some occasions a low-exposure flat was also employed. The combined effect of the instrumental response and the colour of the radiation source made a range of signal levels available, which was particularly large for the blue setting. The range was further augmented by utilizing also the faint scattered light outside the slit area. Both the subtraction and division of flats gave similar statistics and the method of division was adopted. Statistics was obtained by division of two well-exposed flats, and by the division of the lower exposure flat with one of the well-exposed ones.

The initial estimates of G and B were obtained by a linear regression analysis, and were improved iteratively using the Marquardt algorithm. Equation (3) was fit both in the linear domain and in the logarithmic domain. In the case of spectroscopy flats, σ and S were transformed as given by Equation (5). Fits were attempted by including as well as neglecting the quadratic term. In general, the logarithmic fit was better as it passed through the bias values closely. It was noticed that whenever the quadratic term was negligible the fit tended to yield a negative value for the last coefficient. In such cases, as also whenever the value of the coefficient was less than its formal error, it was decided to use the fit that neglects the quadratic term.

The Statistical data and the adopted fits are shown in Figs 1–5, and the final results are presented in Table 1. The formal errors of G and B are < 1 per cent. The imaging flats yield a slightly higher value of G even when the quadratic term is included. It is apparent that even though flat-fielding is done to an accuracy of ≤ 1 per cent, the variance contains the effect of flat-field to the level of ~ 1 per cent. On the other

Table 1. System gain and readout noise.

Gain setting	Method	B electrons	G DN electron^{-1}	Q electron DN^{-1}
Photometrics:				
0	S	17.40	0.0361	27.71
		0.15	0.0002	0.17
	I	17.90	0·0367	27.26
		0.10	0.0001	0.09
33	S	12.26	0.0729	13.72
		0.10	0.0005	0.09
	I	11.85	0.0761	13.15
		0.10	0.0004	0.07
66	S	10.94	0.1105	9.05
		0.10	0.0010	0.08
100	S	11.52	0.1491	6.71
		0.06	0.0007	0.03
500	S	19.91	0.6469	1.55
		0.13	0.0043	0.01
Astromed:				
9.2	S	7.78	0.2410	4.15
		0.04	0.0011	0.02
	I	7.70	0.2517	3.97
		0.15	0.0043	0.07

Notes:
Formal errors of the fit appear below the values.
Method: S = spectroscopic flats: I = images flats.

hand, the spectroscopic data always yielded a satistically insignificant, slightly negative value for the quadratic term, exemplifying the advantage of using the more rigorous Equation (5).

In the case of zero cgain (Fig. 1), the variance shows appreciable departure from the standard curve at high signal levels. Such a behaviour is noticed in CCDs as the full-well saturation is approached, though the range of electron levels over which the effect is apparent varies (Mackay 1986). At 27.7 electrons DN^{-1}, the departure in the present case sets in at ~ 140,000 electrons and becomes pronounced at 250,000 electrons. The data beyond 5000 counts was hence not used in the analysis. On the other hand, Mayya (1991) finds using flats exposed to the level of 2.7–4.1 x 10^5 electrons per pixel, that the CCD is linear to an accuracy of 1 per cent over signal levels 8,200–300,000 electrons. The full-well capacity of the chip is expected to be 500,000 electrons (McCall, English & Shelton 1989).

The variance was generally found to be larger than predicted by the fit for $s \leqslant 5000$ electrons at all gain settings. The statistics at these signal levels was derived from the first 100 rows of the CCD frames. Mayya (1991) had found that stars recorded in this region showed appreciable departure form the standard magnitudes. A possible reason for these departures is the deferred charge nonlinearity, or the poor charge transfer efficiency (CTE) of the Thomson-CSF chip at low light levels (*cf.*, McLean 1989). The effect is more pronounced in the early rows, and vanishes after initial transfers leave back sufficient amount of charge in the pixel to overcome the inefficieny.
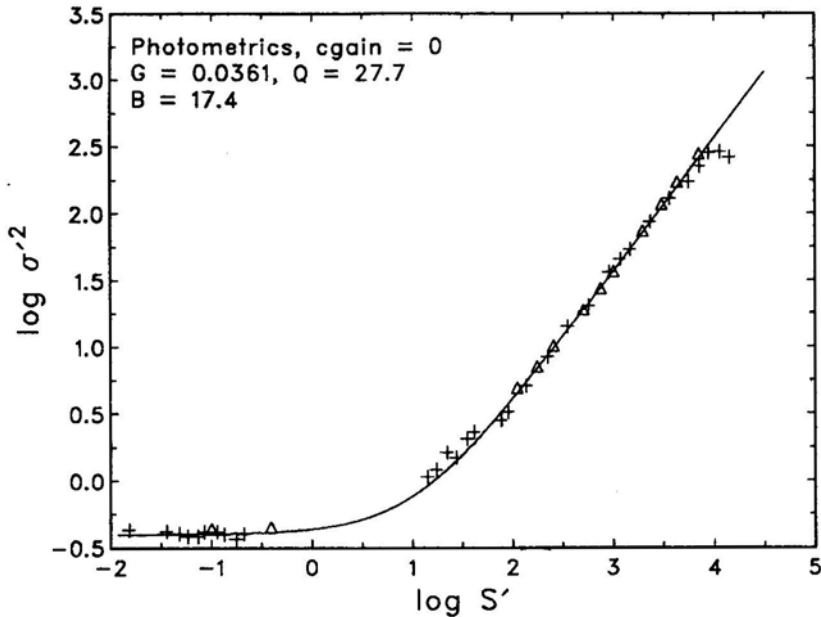
Figure 1. The logarithmic plot of variance versus signal together with the theoretical fit for the Photometrics CCD system at cgain = 0. The points based on spectroscopic flats (+) and imaging flats (Δ) are separately shown. Here, and in the subsequent plots, only selected points are shown for clarity, whereas a large number of points were used in deriving the fit; also the variance of bias counts is shown as log $S < 0$. The fits pass through the large S points better since the full data set used for the fit had a large number of points there. The fit is based on spectroscopic data in the range $150 \leqslant S \leqslant 5000$, and the bias statistics. The nonlinear behaviour of noise for $S > 5000$ counts is evident. Note that the noise is higher than expected at low signal values.

This nonlinearity can be overcome by preflashing. An alternative source of noise is the division by small numbers when two nearly equally exposed flats are used (McCall, English & Shelton 1989).

The base-level noise B includes, in addition to the readout noise R, truncation noise due to digitization of the analog data from the CCD chip and noise due to pick-up from external signals. The contribution to the base-level variance due to truncation is $T^2 = (Q^2 - 1)/12$ (Newberry 1991). The values listed in Table 1 decrease with increasing gain between $0 < \text{cgain} < 66$, showing that such an effect is likely. The estimates of readout noise corrected using Newberry's prescription are 15.5, 11.6 and 10.6 electrons, respectively, for cgain = 0, 33 and 66. The values continue to decrease with increasing gain. The readout rate decreases with increasing cgain as described below and we ascribe the decrease in the readout noise from cgain = 0 to 66 to this fact.

The high value of B at cgain = 500 is due to external pickup. The pick-up appears as faint vertical strips at cgain = 0. As the gain is increased, the image data acquisition control increases the preamplifier gain and also reduces the readout rate. The strips become more pronounced, wider, and inclined. A pattern of spikes sometime becomes visible at cgain > 33. The pick-up was seen to be variable, and the source has since been identified and removed. In order to understand the nature of the pick-up, the following experiments were performed using the frames that showed significant pick-up.
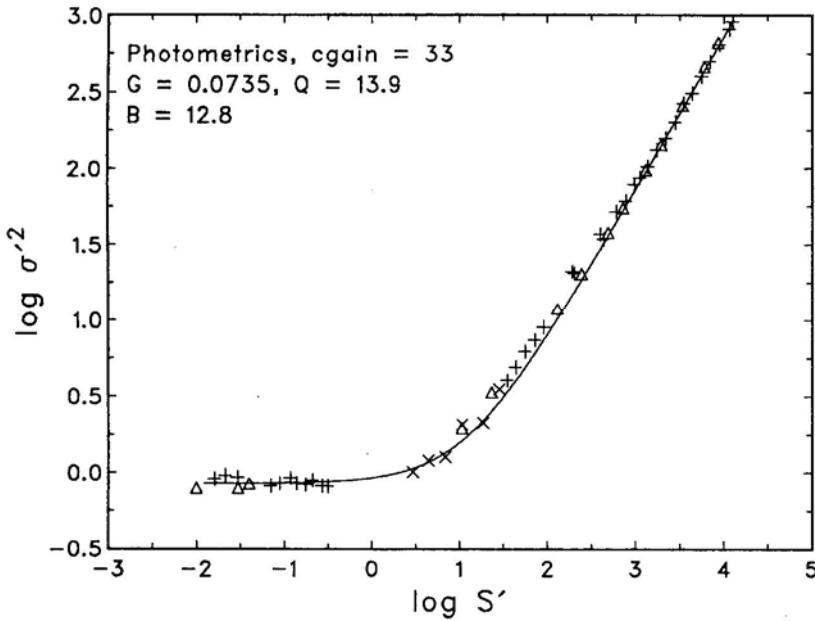
Figure 2. The logarithmic plot of variance versus signal together with the theoretical fit for the Photometrics CCD system and cgain = 33 based on the data obtained in 1992 January. The fit is based on spectroscopic data in the range $300 \leqslant S \leqslant 10000$, and the bias statistics. Other details are as in Fig. 1. Surprisingly, data from a different set ($\times$) obtained on 1991 May 12, agrees with the theoretical fit even at low signal values.
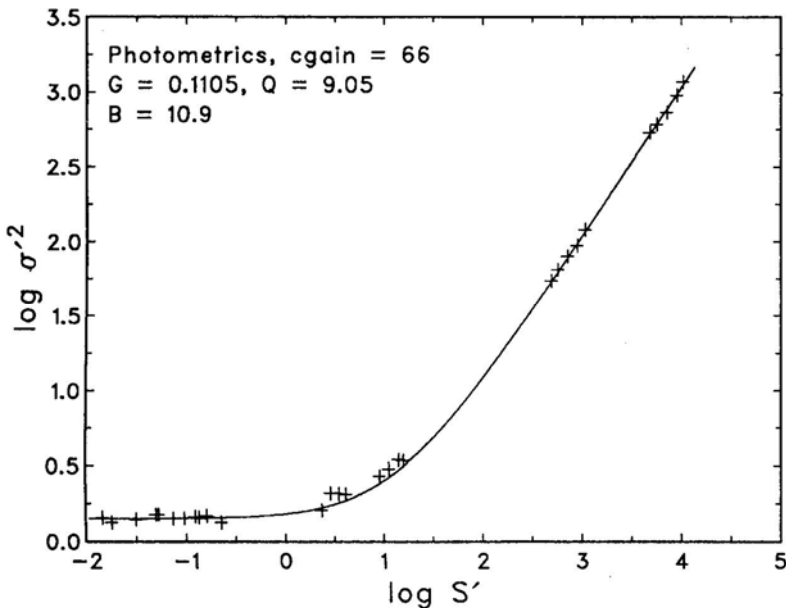

Figure 3. The logarithmic plot of variance versus signal together with the theoretical fit for the Photometrics CCD system and cgain = 66. The fit is based on data in the range $S > 500$, and the bias statistics. Other details are as in Fig. 1.
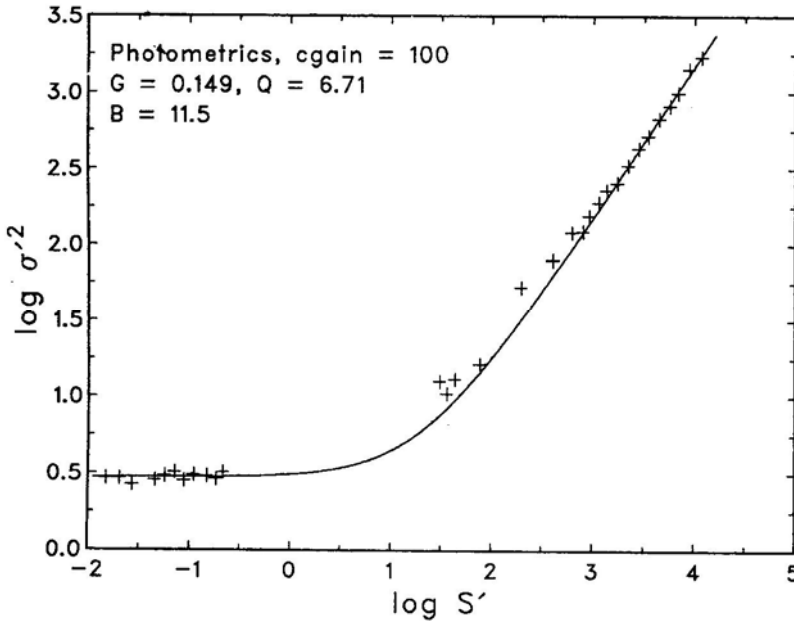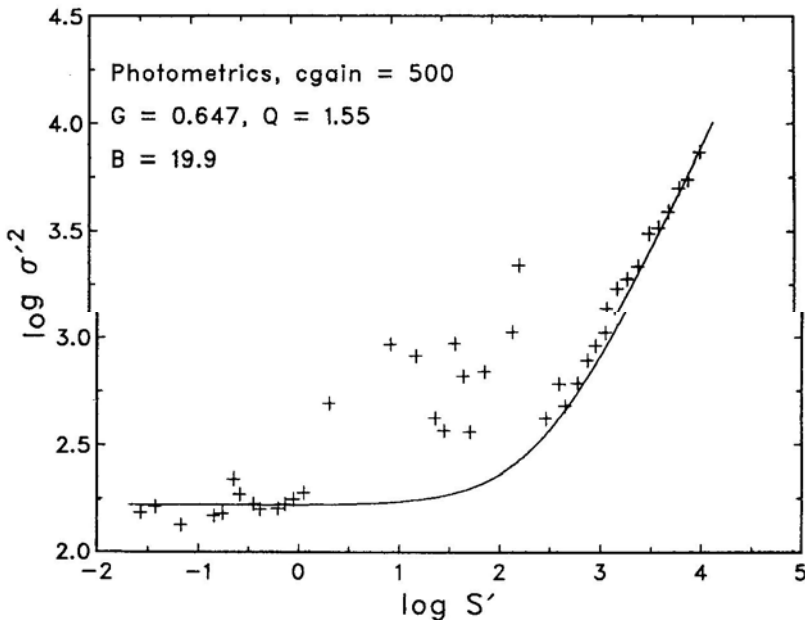
Figure 4. The logarithmic plot of variance versus signal together with the theoretical fit for the Photometrics CCD system and cgain = 100. The fit is based on data in the range $S > 600$, and the bias statistics. Other details are as in Fig. 1.

Figure 5. The logarithmic plot of variance versus signal together with the theoretical fit for the Photometrics CCD system and cgain = 500. The fit is based on data in the range $S > 3000$, and the bias statistics. Other details are as in Fig. 1. Note the discordant data for S = 1 − 100 counts (1 − 150 electrons), which is probably due to the low-level charge transfer inefficiency (the 'deferred charge' problem).
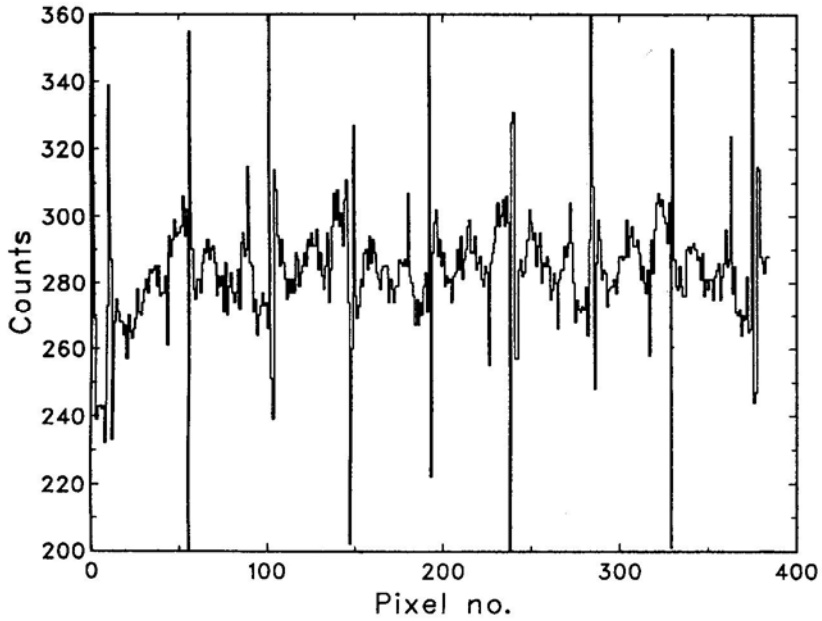
T. P. Prabhu et al.

Figure 6. Data from row 101 of a bias frame obtained at cgain = 500 showing the modulation due to 50 Hz mains pick-up. The spikes often extend a little beyond the limits plotted.
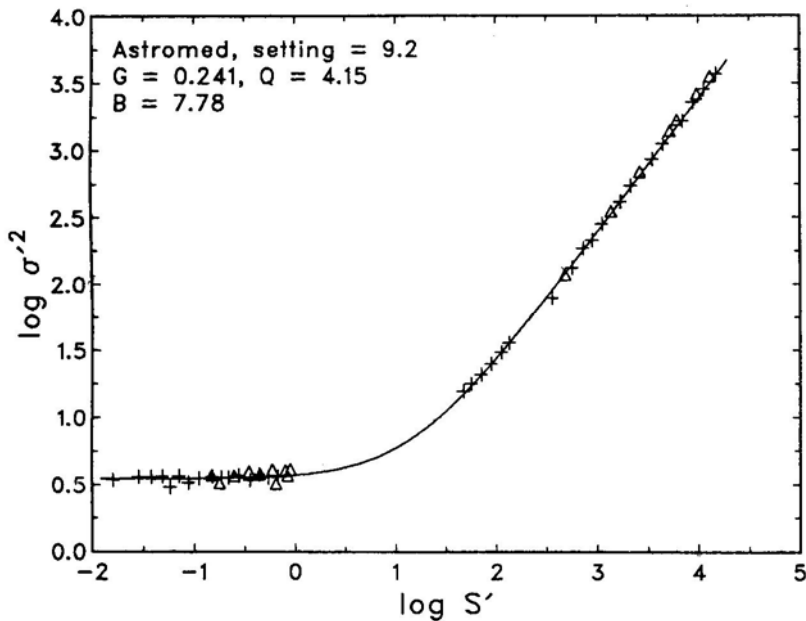

Figure 7. The logarithmic plot of variance versus signal and the corresponding theoretical fit for the Astromed CCD system at gain setting of 9.2. The symbols are as in Fig. 1.

First, the bias frame transfer times were measured to determine approximate readout rates. They were 4.9, 7.9, 10.9, 13.9, 49.4 and 94.0s, respectively, at cgain = 0, 33, 66, 100, 500 and 1000. These values fit a linear relation

$$\text{transfer time(s)} = (4.96 \pm .03) + (0.08901 \pm .00004)\text{cgain}, \qquad (8)$$

with a correlation coefficient of 0.999999. Next, an 8192 point series of data was picked beginning from the first column of row 101. An examination of the data for cgain = 0 showed that spikes repeat with a period of 45 pixels (Fig. 6). However, alternate spikes have positive and negative deviations compared to the mean bias. There is also an almost sinusoidal pattern seen with 90 pixel periodicity, and 15 count amplitude. Superposed on this is a wave with a periodicity of about 18 pixels. The first three pixels of each row, which showed counts higher than average, were then replaced by mean counts and the power spectrum of the series was obtained for cgain = 33, 100 and 500. Two strong periods were seen at 18.1 and 90.7 pixels. Additional periodicities were also seen at 10.0,13.0 and 30.2 pixels. A similar pattern was evident at other values of cgain also, but with periods 3.66 and 6.49 times at cgain = 100 and 33, respectively. These factors are in a general agreement with the measurements of frame transfer times. The pick-up is hence due to the same source at all values of cgain; but the power in these periodicities falls quickly as the gain is reduced.

The manual for DIPS 1000 system informs that the readout rate is 50 kHz. If one assumes that this rate corresponds to the default value of cgain, the derived frequencies of pickup turn out to be close to 50 Hz and its harmonics. Assuming the 50 Hz mains to be the source, the derived readout rates are 29.4, 16.6 and 4.53 kHz at cgain = 33, 100 and 500, respectively. These results also follow a linear relationship which can be expressed as

$$\text{readout time per pixel } (\mu s) = (20.5 \pm 0.2) + (0.4003 \pm 0.0005)\text{cgain}. \qquad (9)$$

For a format of 384×576 pixels, this agrees well with Equation (8). The exact mains frequency was not measured at the time of these experiments. It is known to vary between 48 and 51 Hz, though close to 50 Hz most often.

The amplitude of the spikes is about 60, 14, and 3 counts at cgain = 500,100 and 33, respectively. These can easily be rejected from the data, and were hence not considered while deriving the statistics. The underlying smooth variation at 50 Hz has an amplitude of 15 and 1 counts at cgain = 500 and 100, respectively, whereas it is hardly noticeable at cgain = 33. The pick-up increases the base-level noise significantly at cgain =100 and dominates at cgain = 500. Some effect could still be present at cgain = 66.

The system gain G listed in Table 1 appears to increase almost linearly with the parameter cgain. Since the parameter is software selectable and changes both the amplifier gain and the readout rate through internal programme, the relationship may not necessarily be linear. A polynomial fit to the data in Table 1 which serves as an interpolation formula is

$$G = (0.0358 \pm 0.0005) + (0.001111 \pm 0.000001) \text{ cgain} + (2.2 \pm 0.1) \, 10^{-7} \text{ cgain}^2 \quad (10)$$

with a standard error of 0·0005. An extrapolation to cgain = 4095 (which is certainly not justified) yields a value of G = 8.3 DN electron^{-1}, and a value of $G \simeq 1$ DN electron $^{-1}$ is reached for cgain ~ 750.

3.2 *The Astromed System*

The Astromed system was calibrated using the IIA CCD dewar and the TIFR controller. The amplifier gain was set to 9.2. Flats were obtained in 1991 March using a laboratory set-up to expose the CCD to diffuse daylight without using any filter. Altogether 21 graded flats were obtained with averge signal varying from 500 to 28300 counts above bias. The flats were interspersed by bias frames. Eleven best exposed flats were stacked to obtain the master flat; the remaining 10 were corrected using the master. The procedure for gain calibration was generally similar to the one with the imaging flats of Photometrics CCD system described earlier. The spectroscopic flats were obtained as a part of an observational programme on novae and galaxies on 1991 March 10 and 11. The Boller & Chivens spectrograph with a 3001 mm^{-1} grating and a 6-inch camera were used. The wavelength range covered was 4400–7000 Å. A whitened particle board fixed on the dome and illuminated by tungsten filament lamp was used as the source. The procedure of analysis was the same as for the Photometrics system described earlier. The results are presented in Table 1, and the fit is shown in Fig. 7. The data from scattered light in the range of 150–700 electrons also fit the theoretical curve well, indicating that the effect of the deferred-charge threshold is less important for this chip. The GEC chip is known to be good up to 25 electrons (McLean 1989). Mains pick-up was not evident in the bias frames, and the truncation noise is low at this gain. Hence the readout noise is likely to be close to 7.8 electrons.

Using a different chip available with TIFR unit in 1990, a value of $Q = 1.12$ was obtained for the amplifier setting of 34 (Bhat *et al.* 1991, in preparation). The preamplifier settings in the Astromed controller can be varied between 2 and 69 in a few discrete steps. The present results suggest that one obtains about 19 electron DN^{-1} at the gain setting of 2, and the total range of the ADC would then be about 624,000 electrons including the bias. At the gain of 69, on the other hand, one expects 0.5 electrons DN^{-1}. The optimal system gain would be at the setting of 4.9 giving 7.8 electrons DN^{-1}. The full-well capacity of the GEC chip is > 100,000 electrons, and typically 300,000 electrons. The saturation is reached within the limit of the ADC at the lowest gain setting.

4. Conclusions

The main conclusions of this work are listed below.

1. *The method of analysis*: The system gain, readout noise, and the threshold of a CCD can all be determined by studying the noise characteristics of a CCD image. The method of using graded flats, correcting for bias, dark if any, and flat-field response, is satisfactory. On the other hand, the method of using division of two flats, or substraction of two normalized flats, together with the signal and noise transformation of Equation (5), is more rigorous. The final fit giving base-level noise, system gain, and residual flat-field variation can be determined more accurately using the Marquardt alogorithm rather than the conventional regression fit. The RESPECT commands GSTAT and GFIT enable the evaluation of the statistics, and the computation of the fit, respectively, using a small number of low-resolution spectroscopic flats.

2. *The system gain*: The inverse system gain Q for the Photometrics system varies from 27.7 electrons DN^{-1} at cgain = 0 to 1.55 electrons DN^{-1} at cgain = 500. The value of 9.1 electrons DN^{-1} at cgain = 66 agrees with the determination of McCall, English & Shelton (1989) for a similar system. This gain setting is optimal for most of astronomical observations requiring good sensitivity as well as large dynamic range. The Astromed unit with the IIA data acquisition system at the VBT has Q = 4.15 electrons DN^{-1} at the gain setting of 9.2. The preamplifier gain may be reduced further by a factor of 2 for optimizing the system. On the other hand, the IIA Controller has been exhibiting 'binning bias' (Djorgovski 1984) in recent years, which has rendered the base-level noise higher by a factor of 2–3. Hence it is advisable to continue with this gain setting until the problem is rectified. The loss in dynamic range is not significant since the output has an extra bit available (maximum counts 32767).

3 *The readout noise:* The readout noise is estimated as $\leqslant 11$ electrons for the Thomson-CSF 7882 CDA chip, and ~ 8 for the GEC P8603 chip. The models of noise in the data require the base-level noise which include, in addition to the readout noise, also the external source of noise. The readout noise itself increases with increasing readout rate. The base-level noise needs to be computed for each data set experimentally.

4. *Nonlinearity*: The Thomson-CSF chip shows nonlinearity in the variance diagram at signal levels below 10,000 electrons and above 150,000 electrons. Photometric studies have however shown the chip to be linear at least over the range of 8,000–300,000 electrons. Further investigations are needed to understand the behaviour at low and high signals. At the lowest signal levels ($\leqslant 150$ electrons) the chip is affected by deferred-charge threshold. This can be alleviated by preflashing to the level of 100 electrons per pixel (*cf.*, McCall, English & Shelton 1989). The effect of threshold was not detectable for the GEC chip which is known to be good above 25 electrons (McLean 1989).

Acknowledgments

References

Ananth, A. V., Srinivasan, R., Srinivasulu, G., Chandramouli, S. S. 1991, *Indian J. Pure Appl. Phys.,* **29**, 529.

Bhat, P. N., Kembhavi, A. K., Patnaik, K., Patnaik, A. R., Prabhu, T. P. 1990, *Indian J. Pure Appl. Phys.,* **28**, 649.

Djorgovski, S. 1984, in *Proc. Workshop Improvements to Photometry,* Eds W. J. Borucki & A. Young, NASA CP-2350, p. 152.

Horne, K. 1988, in *New Directions in Spectrophotometry,* Eds. A. G. D. Philip D S Hayes & S. J. Adelman, L. Davis Press, Schenectady, p. 285.

Mackay, C. D. 1986, *A. Rev. Astr. Astrophys.,* **24**, 255.

Mayya, Y. D. 1991, *J. Astrophys. Astr,* **12,** 319.

McCall, M. L., English, J., Shelton, I. 1989, *J. R. astr. Soc. Canada,* **83**, 179.

McLean, I. S. 1989, *Electronics and Computer-aided Astronomy,* Ellis Horwood, Chichester.

Newberry, M. V. 1991, *Publ. astr. Soc. Pacific,* **103**, 122.

Prabhu, T. P., Anupama, G. C. 1991, *Bull. astr. Soc. India,* **19** (in press).

Press, W. H., Flannery, B. P., Teukolsky, S. A., Vetterling, W. T. 1986, *Numerical Recipes,* Cambridge Univ. Press.

Sagar, R., Pati, A. K. 1989, *Bull. astr. Soc. India,* **17**, 6.